



# Journal of Applied Sciences

ISSN 1812-5654

**science**  
alert

**ANSI***net*  
an open access publisher  
<http://ansinet.com>

## Characterization of the Structure Feature of Bimetallic Fe-Ni Catalysts

<sup>1</sup>S.E. Eliana Misi, <sup>2</sup>A. Ramli and <sup>3</sup>F.H. Rahman

<sup>1</sup>Department of Chemical Engineering,

<sup>2</sup>Department of Fundamental and Applied Sciences,  
Universiti Teknologi PETRONAS, Bandar Seri Iskandar, 31750 Tronoh,  
Perak Darul Ridzuan, Malaysia

<sup>3</sup>Petronas Research Sdn Bhd, Jalan Ayer Itam, Kawasan Institusi Bangi,  
43000 Kajang, Selangor Darul Ehsan, Malaysia

**Abstract:** Production of hydrogen gas from biomass gasification usually comes with several problems such as the existence of unacceptable level of tars and also ineffectiveness of the catalysts performance due to coke deposition. In order to eliminate most of the inconvenience encountered, new types of catalyst have been developed. In this study, bimetallic Fe and Ni supported on zeolite beta have been prepared by incipient wetness impregnation method with different calcination temperatures (500-700°C). The interaction of active metals and support on the structure, metals transition and reduction were characterized by physicochemical techniques such as BET, XRD, FESEM-EDX and TPR. The results showed that the active metals incorporated with zeolite beta in bimetallic systems exhibit a strong Fe-Ni/BEA interaction, which stabilises Fe<sup>3+</sup> and Ni<sup>2+</sup> ions in the lattice. Reducibility of nickel increased in the presence of Fe, which was confirmed by the combination of active metals reduction peaks attributed to weak interaction with the support, Fe<sub>2</sub>O<sub>3</sub> to Fe<sub>3</sub>O<sub>4</sub> to FeO and strong interaction with the support between FeAl<sub>2</sub>O<sub>4</sub> and NiAl<sub>2</sub>O<sub>4</sub>. Bimetallic catalysts have a bigger surface area with increasing calcination temperatures, which is closely related to high activity in the gasification reaction. It was found that different calcination temperatures give a significant effect to the precursor whereby Feni/BEA (600°C) showed better physicochemical properties than other samples with high reducibility even though it has low surface area.

**Key words:** Biomass, gasification, catalyst, bimetallic, zeolite beta, iron, nickel

### INTRODUCTION

The production of hydrogen from gasification of biomass as an alternative fuel for transportation, power generation and chemical feedstock is the principal part of the effort to meet the goal of a biomass-based technology. The development on this process was started over century ago and has sustained into the present. However, this effort is allied with a number of problems (Asadullah *et al.*, 2003). The main problem is the formation of solid residues consisting of char, ash, volatile alkali metals and tar (Uddin *et al.*, 2008) which is very harmful and limits the hydrogen production. Moreover, the continual build up of tar present in produce gas can cause blockage and damage to the equipment which can reduce the efficiency of the gasification system (Sutton *et al.*, 2001).

Recently, interest has grown on the subject of catalysis of biomass gasification to eliminate tar in the

product and emphasize on the production of hydrogen-rich gas (Hu *et al.*, 2006). Among Ni, Co, Fe, Ru and Pt catalyst, supported Rh catalyst showed best performance in steam gasification. It was demonstrated that catalysts having a loading of  $1.2 \times 10^{-4}$  (Rh)/g-cat can convert 98-99% of the carbon in biomass to products at 873 K (Asadullah *et al.*, 2003). For economic reason, nickel and iron based catalysts were still the preferred choice due to their wide availability and cheapness (Uddin *et al.*, 2008; Zhang *et al.*, 2007). Several nickel based catalysts have been investigated and found to be very active in destruction of tar (Sato and Fujimoto, 2007). However, the activity of the catalyst is sensitive to nickel loading and metal dispersion (Sutton *et al.*, 2001). The reaction is frequently accompanied by coke formation and sintering of Ni metal particles, leading to catalyst deactivation.

Iron catalyst, which contains hematite Fe<sub>2</sub>O<sub>3</sub>, is also active in reforming hydrocarbon and diminishes the tar content in the gas mixture. According to the previous

study (Nordgreen *et al.*, 2006) when metallic Fe is utilised as tar-depleting catalyst in the gasification of biomass, the product gas has significantly lower tar content. Furthermore, surface area of the iron oxide catalyst played an important role in the catalytic tar decomposition. It was found that the addition of  $\text{Al}_2\text{O}_3$  to iron oxide was one method for the improvement of the surface area without deactivation (Uddin *et al.*, 2008).

In order to provide high catalytic reaction in biomass gasification, the usage of a bifunctional bimetallic catalyst consisting of active metal and an acidic zeolite beta or so-called International Zeolite Association Framework Designation: BEA has been focused in this study. BEA has been used as support for several catalysts because of their molecular sieve properties as well as shape selective characteristic and excellent acid support (Jordao *et al.*, 2007). It has also been reported that some significant advantages can be added when amorphous support was replaced with crystalline materials such as zeolite or BEA. Selectivity will be improved due to higher density of acidic sites present in the zeolite, higher activity during reaction and additional resistance to sulphur poisoning (Jordao and Cardoso, 2001).

In this study, BEA supported bimetallic Fe-Ni in which Fe and Ni are compatible elements has been prepared at different calcination temperatures. The objectives of this study are to identify the changes caused in the properties of these catalysts by the insertion of a second metal and effect of calcination temperatures to the precursor. This is because the variation of the catalysts properties can reflect the interaction among metal and support and also the agglomeration features of the active sites on the metal catalyst.

## MATERIALS AND METHODS

**Catalyst preparation:** For the preparation of bimetallic catalysts, the metals were loaded into the support via a two-step incipient wetness impregnation method. For the first step impregnation, 5wt% metal loading of Ni based catalysts was prepared. First, BEA as the supported is calcined at 500°C for 16 h. Then, a required amount of  $\text{NiCl}_2 \cdot 6\text{H}_2\text{O}$  was dissolved in sufficient amount of distilled water followed by adding 95% of BEA to the metal salt solution under continuous stirring. The slurry formed will be left for impregnation for 4 h under stirring and later dried at 120°C for 16 h. Finally, the dried samples will be calcined at 500-700°C for 16 h. The second metal is introduced in the second impregnation step using another 5 wt% of Fe metal, yielding 5%Fe5%Ni/BEA which is

designated as FeNi/BEA where in YX/BEA (T°C), metal X is impregnated first, followed by metal Y and T is calcination temperature.

**Catalyst characterization:** BET surface area, volume and BJH pore size distribution of the bimetallic catalysts were determined by  $\text{N}_2$ -physisorption using micromeritics ASAP 2000 apparatus at liquid- $\text{N}_2$  temperature of -196°C. The samples were degassed under nitrogen at 120°C for overnight before they were analyzed. The Powder X-ray Diffraction (XRD) patterns were obtained using a Bruker diffractometer using  $\text{Cu-K}\alpha$  radiation to identify the crystalline phases and crystallite size of FeNi/BEA catalysts. The Temperature Programmed Reduction (TPR) experiments were performed to determine the reducibility of the metal present on the catalyst surface and investigate interaction between the metal and support. The TPR runs utilized 5% $\text{H}_2$  / $\text{N}_2$  with a flow rate of 20  $\text{cm min}^{-1}$ , and the temperature was programmed to increase at a rate of 10°C  $\text{min}^{-1}$  from room temperature to 800°C. Field Emission Scanning Electron Microscopy (FESEM) analysis was conducted to study the morphology of the catalysts.

## RESULTS AND DISCUSSION

**Textural properties of catalyst:** BEA has tridirectional system of interconnected channels (Kang *et al.*, 2008) with 12-ring orifice and 3D pore structure (Chen *et al.*, 2006) providing large and small cavities. The frameworks are composed of  $\text{SiO}_2$  and  $\text{Al}_2\text{O}_3$ . Based on  $\text{N}_2$ -physisorption terms, the textural properties like BET surface area and pore volume of the catalysts prepared using BEA as support were calculated and summarized in Table 1 and their pore size distribution patterns are shown in Fig. 1.

Table 1 shows that the surface areas of the catalysts are varied widely where fresh BEA has bigger surface area 529.04  $\text{m}^2 \text{g}^{-1}$  compared to the bimetallic catalyst. Once BEA is incorporated with active metals, the surface area is reduced. The decrease in the surface area of the bimetallic catalysts are 15.8, 16.5 and 15% in the case of after calcinations at 500, 600 and 700°C, respectively. The influence is so pronounced in some instances that Fe and Ni have occupied the BEA pore which resulted in the surface area reduction. Catalysts with more available surface area generally are more active, more adsorptive, sinter at lower temperature and exhibit more catalytic activity (Webb and Orr, 1997). Moreover, the surface area of the catalyst is identical with the pore volume where the size of pore volume is reduced when more active metals were impregnated with BEA.

**Table 1: Textural properties of the catalysts**

Temperature (°C)	Catalysts	BET surface area (m <sup>2</sup> g <sup>-1</sup> )	Pore volume (cm <sup>3</sup> g <sup>-1</sup> )
500°C	BEA	529.043	0.151
	FeNi/BEA	445.446	0.123
600°C	FeNi/BEA	441.816	0.124
700°C	FeNi/BEA	449.752	0.093

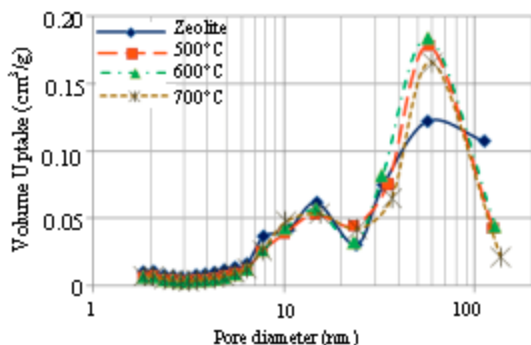


**Fig. 1: Pore distribution of the catalysts**

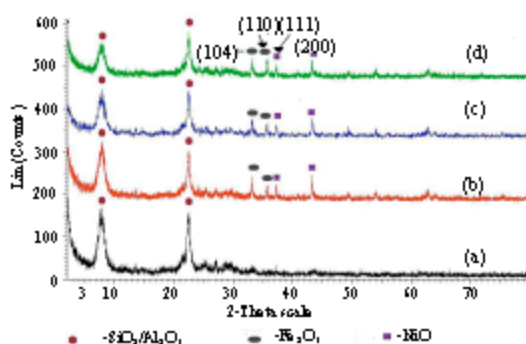


**Fig. 2: XRD patterns for (a) BEA and FeNi/BEA calcined at different calcination temperatures (b) 500°C (c) 600°C (d) 700°C**

In the present study, the composite of FeNi/BEA is found to exhibit a wide pore distribution plot (Fig. 1) which scattered in the mesopores region, 2-50 nm and macropores region from 50 to 130 nm. Nitrogen volume uptake increased as number of pores was increased in the range of 20-60 nm when BEA was incorporated with active metals. Hence, high BET surface area, high pore volume and wide pore distribution of the bimetallic catalysts in terms of  $N_2$ -physorption may be closely related in promoting high activity in the gasification reaction.

**Powder X-ray diffraction:** The XRD patterns of the prepared catalysts via incipient wetness impregnation method with different calcination temperatures are

displayed in Fig. 2. Both active metals revealed two diffraction peaks, which are corresponding to hematite,  $\alpha$ -Fe<sub>2</sub>O<sub>3</sub> phase and bunsenite, NiO phase, respectively.

The peaks for iron phase with the appearance of (104) and (110) plane positioned at the  $2\theta$  of 33.1° and 35.6° meanwhile for NiO phase with the appearance of (111) and (200) plane at the  $2\theta$  of 37.3° and 43.3°. These planes are in agreement with data reported in the JCPDS index and from previous study (Kang *et al.*, 2008; Rynkowski *et al.*, 1993; Zielinski, 1982). The peaks for BEA which appeared as a major plane were at the  $2\theta = 8^\circ$  and  $22.5^\circ$ . The intensity of fresh BEA diffraction peaks was high and quite broadening illustrating that the peaks contain SiO<sub>2</sub> and Al<sub>2</sub>O<sub>3</sub>. However, when FeNi was incorporated with BEA, the intensity of BEA diffraction peak became lower and shifted to higher  $2\theta$  value. This may due to the formation of interacted species between iron and nickel with alumina or silica in BEA. However, formation of nickel aluminate and iron aluminate phase have not detected probably due to the lack of crystallinity as observed previously by Zielinski (1982) and confirmed by Salagre *et al.* (1996).

Temperature is one of the important factors, which influence the product components and shapes where it can break up the precursor and eventually decelerates the crystallization. Referring to the prepared catalysts with different calcination temperatures from 500 to 700°C, characteristic lines towards lower value of  $2\theta$  as well as their intensities were slightly shifted due to the agglomeration of the particles. The situation is obviously in the case of BEA wherein the diffraction peaks were decreased with increasing of calcination temperatures. This indicates that the temperature has also contributed to the crystallization of the prepared catalysts. Referring to the JCPDS index, the bimetallic catalysts had hexagonal structure (89-5416) for Fe<sub>2</sub>O<sub>3</sub> and cubic structure (47-1049) for NiO, respectively.

The crystallite size of the catalysts can be estimated based on the basis of line broadening analysis using Scherer's formula. The calculation was relied on the intensity value of the main metal peak. It can be clearly observed that the bimetallic catalyst has greater particle size when calcined at higher temperature, 700°C. This could be due to agglomeration of the active metals after prolonged treatment at high temperature.

**Field emission scanning electron microscopy:** The morphology of the prepared catalysts was examined by FESEM and the images are displayed in Fig. 3. From the Fig. 3a, the BEA which is a conventional catalyst has been determined in fine particles with indistinct features.

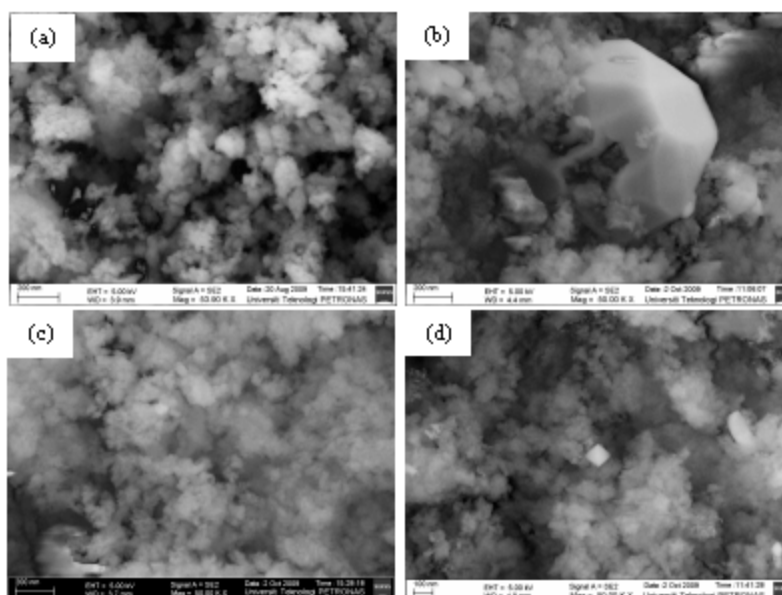


Fig. 3: FESEM images of the prepared catalysts (a) BEA and FeNi/BEA at different calcination temperatures (b) 500°C (c) 600°C (d) 700°C

Table 2: Crystallite size of the catalyst (nm)

Samples	500°C	600°C	700°C
<b>FeNi/BEA</b>			
Ni	104.91	77.66	106.52
Fe	87.25	91.62	93.45

Table 3: EDX data for bimetallic catalysts

Temperature (°C)	Catalyst	Element (Weight %)				
		Si	Al	O	Fe	Ni
500	BEA	41.9	3.3	54.8	-	-
	FeNi/BEA	37.3	2.6	52.4	4.6	3.2
600	FeNi/BEA	33.4	2.6	57.3	3.2	3.5
	FeNi/BEA	40.3	2.9	48.9	5.2	2.7

When BEA impregnated with bimetallic structure and calcined at 500°C, the prepared catalysts revealed a crystalline phase instead of indefinite features. The crystalline phase with hexagonal structure was referring to  $Fe_2O_3$ , the second metal in bimetallic catalyst as confirmed in XRD characterization. Thus, this ascribed to the fact that the  $Fe_2O_3$  crystalline phase submitted little contribution to the metal dispersion resulting less interaction with nickel and support. Particularly, too high iron loading results in the formation of  $Fe_2O_3$  crystalline phase on the support. However, the crystallization was improved after calcination at 600°C but decreased at 700°C where a minor crystalline phase can still be observed.

The surface elemental compositions of the prepared catalysts were characterized by EDX analysis and the results are shown in Table 2. Fe and O have been detected verifying the prepared catalyst is in the form of hematite,

$Fe_2O_3$  phase which validate the XRD analysis. Meanwhile Ni and O confirm that the catalyst is in the form of nickel oxide, NiO phase and Si-O with Al-O in the form of BEA. When the Fe and Ni were impregnated together with BEA, it shows that both phases were present in the bimetallic catalysts. The weight percentage for both metal are different where the first metal loading with support has less percentage compared to second metal. This implies that the second metal has covered the first metal during the impregnation Table 3.

**Temperature Programmed Analysis ( $H_2$ TPR):** Figure 4 shows the TPR profile of the catalysts calcined at 500°C with Ni/BEA and Fe/BEA which were used as standard. The reduction of 5%Ni/BEA gives two stages with peak maxima at 420 and 590°C, respectively. Zielinski (1982) indicates that the low temperature peak on the TPR curve is due to the reduction of NiO not bound with the support which refers as “free nickel oxide”. Meanwhile the higher temperature peak is corresponded to the reduction of nickel that had reacted with the support forming nickel aluminate,  $NiAl_2O_4$  so-called “fixed nickel oxide”. The formation of this aluminate is possible as a result of the reaction of extra-framework alumina which is present in the zeolite sample. Due to the framework silica/alumina ratio, roughly small amount of alumina that might be present in the sample is outside of the framework and is available for reaction with the nickel oxide to form the nickel aluminate ( $NiAl_2O_4$ ). The XRD

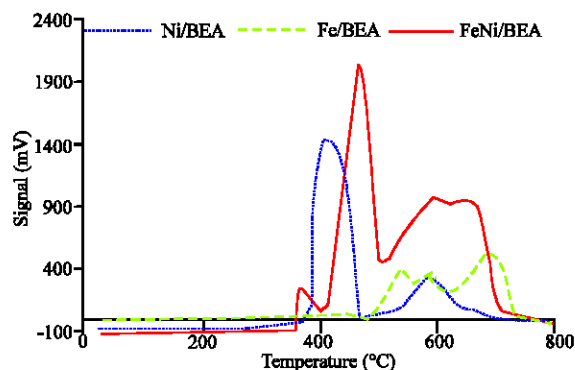


Fig. 4: H<sub>2</sub>-TPR profile of the catalyst at 500°C

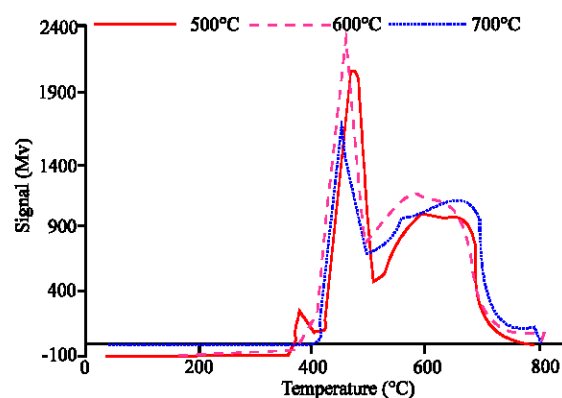


Fig. 5: H<sub>2</sub>-TPR profile of FeNi/BEA at different

data, however, have not shown any diffraction peak for existence of nickel aluminate in the catalyst resulted of low crystallinity.

**Calcination temperatures:** It was found that the preparation procedure such as types of nickel salt used, support and calcination temperature is one of the factors that contributed to the fraction fixed nickel oxide development (Zielinski, 1982). The reduction profile of 5%Ni/BEA is in accordance with Cheng *et al.* (2001) where nickel in NiO is reducible below 500°C while nickel in NiAl<sub>2</sub>O<sub>4</sub> is reducible above 500°C or 600°C.

The phase transformations of 5%Fe/BEA during TPR process showed three stages (between 500°C-800°C) with the existence of several reduction phases of iron oxide, which might be attributed to weak interaction of the support, Fe<sub>2</sub>O<sub>3</sub> to Fe<sub>3</sub>O<sub>4</sub> and to FeO as confirmed by Wan *et al.* (2007) and strong interaction with support, FeAl<sub>2</sub>O<sub>4</sub>. Reduction of Fe<sub>2</sub>O<sub>3</sub> ends at FeO phase rather than Fe because FeO is a metastable phase of iron oxide on the support (Wielers *et al.*, 1989). The strong interaction between Fe-Al<sub>2</sub>O<sub>3</sub> provided the stabilization of

FeO phase on Al<sub>2</sub>O<sub>3</sub> (Zhang *et al.*, 2006) which could further retard the transformation of FeO to Fe (Wan *et al.*, 2007). It should be noted that a lower broad peak between 300-500°C was observed and as reported by Virginie *et al.* (2008) the peak shows the reduction of free iron oxides.

Interaction of FeNi/BEA (500°C) significantly intensify the peak and shifts the reduction peak into lower temperature where the H<sub>2</sub> consumption increased from 34.31 μmol g<sup>-1</sup> to 41.12 μmol g<sup>-1</sup>. This result is in agreement with feseem analysis where the morphology of the FeNi/BEA (500°C) catalyst shows a hexagonal structure of Fe<sub>2</sub>O<sub>3</sub> located on the support. However, the peak gradually disappeared at 600 and 700°C calcinations temperature (Fig. 5). These types of oxides are easily reduced and its existence can cause several difficulties during reaction such as sintering and carbon deposition on the catalyst surface which will lead to catalyst deactivation (Virginie *et al.*, 2008).

The variation in the TPR profile of the bimetallic catalysts in Fig. 5 shows the reductions of nickel and iron phase at 500-800°C region were overlapped into a broad peak, which suggested that the stabilization of Fe<sup>3+</sup> and Ni<sup>2+</sup> ions in the lattice. The reduction undergoes process of Fe<sub>2</sub>O<sub>3</sub> to Fe<sub>3</sub>O<sub>4</sub> to FeO, FeAl<sub>2</sub>O<sub>4</sub> and NiAl<sub>2</sub>O<sub>4</sub>. In the case of FeNi/BEA (500°C) the peak itself split into two; the Fe<sub>2</sub>O<sub>3</sub> to Fe<sub>3</sub>O<sub>4</sub> and FeO while NiAl<sub>2</sub>O<sub>4</sub> reduction appeared first as a discrete peak and the second one representing the reduction of FeAl<sub>2</sub>O<sub>4</sub>. A possible reason for this phenomenon is non-homogeneous mixing of Fe-Ni species due to less metal dispersion as reported by FESEM analysis and hence Fe could not promote the reduction efficiently. However, smooth reduction peaks appeared for 600°C and negligible for 700°C calcinations. Consequently, iron facilitates the reduction of nickel when the several reduction phases are well mixed, resulting in the corresponding peaks appearing at much lower temperature.

The reduction peak associated to the reduction of free nickel oxide NiO to Ni<sup>0</sup> shifted towards lower temperature as the temperatures of calcination increases. The H<sub>2</sub> consumption for the reduction of free nickel oxide, NiO to Ni<sup>0</sup> was 500.04, 531.47 and 394.43 μmol g<sup>-1</sup> for the catalysts calcined at 500 to 700°C. Less H<sub>2</sub> consumption were observed for reducing Ni in NiO in the case of FeNi/BEA (700°C) bimetallic catalyst due to agglomeration of the active metal during the impregnation as confirmed by calculating the crystallite size. Meanwhile, the H<sub>2</sub> consumption for second reduction peaks which represent combination of several phases were 445.46, 551.16 and 494.93 μmol g<sup>-1</sup> for 500, 600 and 700°C calcination temperatures, respectively.

## CONCLUSION

BET analysis shows that the insertion of a second metal reduced the surface area of the bimetallic catalyst. However, the higher calcination temperatures of FeNi/BEA catalyst produced higher the surface area. The pore distributions of FeNi/BEA catalysts lie in the mesopores and macropores region with diameter between 2 and 130 nm. Powder XRD revealed both active metals Fe and Ni showed as two diffraction peaks which are corresponding to  $\text{Fe}_2\text{O}_3$  and NiO. FeNi/BEA (500°C) catalysts revealed a hexagonal structure of  $\text{Fe}_2\text{O}_3$  which submitted little contribution to the metal dispersion compared to the catalyst calcined at 600 and 700°C. The profiles obtained from TPR suggest that, for bimetallic catalysts, the presence of iron facilitates the reduction of  $\text{Ni}^{2+}$  cation due to well combination of several reduction phases attributed to weak interaction and strong interaction with the support. Different calcination temperatures give a significant effect to the precursor whereby FeNi/BEA (600°C) shows better physicochemical properties than other catalysts. Eventhough the catalyst has low surface area, it has high reducibility and has an improvement in the crystallization resulting in lower operation system and a more stabilized activity.

## ACKNOWLEDGMENTS

The authors are grateful for the financial support provided by UTP for this research and for granting a postgraduate scholarship to S.E.E.M.

## REFERENCES

- Asadullah, M., T. Miyazawa, S. Ito, K. Kunimori and K. Tomishige, 2003. Demonstration of real biomass gasification drastically promoted by effective catalyst. *Applied Catal. A: Gen.*, 246: 103-116.
- Chen, S., Y. Yang, K. Zhang and J. Wang, 2006. BETA Zeolite made from mesoporous material and its hydrocracking performance. *Catal. Today*, 116: 2-5.
- Cheng, Z.X., X.G. Zhao, J. Li and Q.M. Zhu, 2001. Role of support in  $\text{CO}_2$  reforming of  $\text{CH}_4$  over Ni/ $\gamma$ - $\text{Al}_2\text{O}_3$  catalyst. *Applied Catal. A*, 205: 31-36.
- Hu, G., S. Xu, S. Li, C. Xiao and S. Liu, 2006. Steam gasification of apricot stones with olivine and dolomite as downstream catalysts. *Fuel Process. Technol.*, 87: 375-382.
- Jordao, M.H. and D. Cardoso, 2001. 14-P-36-Characterization of Ni, Pt zeolite catalysts by TEM and EDX. *Stud. Surface Sci. Catal.*, 135: 357-357.
- Jordao, M.H., V. Simoes and D. Cardoso, 2007. Zeolite supported Pt-Ni catalysts in n-hexane isomerization. *Applied Catal. A*, 319: 1-6.
- Kang, S.H., J.K.W. Bae, P.S.S. Prasad and K.W. Jun, 2008. Fisher-tropsch synthesis using zeolite-supported iron catalysts for the production of light hydrocarbons. *Catal. Lett.*, 125: 264-270.
- Nordgreen, T., T. Liliedahl and K. Sjoström, 2006. Metallic iron as a tar breakdown catalyst related to atmospheric, fluidised bed gasification of biomass. *Fuel*, 85: 689-694.
- Rynkowski, J.M., T. Paryjczak and M. Lenik, 1993. On the nature of oxidic nickel phase in NiO/ $\gamma$ - $\text{Al}_2\text{O}_3$  catalysts. *Applied Catal. A*, 106: 73-82.
- Salagre, P., J.L.G. Fierro, F. Medina and J.E. Sueiras, 1996. Characterization of nickel species on  $\gamma$ -alumina supported nickel samples. *J. Mol. Catal. A*, 106: 125-134.
- Sato, K. and K. Fujimoto, 2007. Development of new nickel based catalyst for tar reforming with superior resistance to sulfur poisoning and coking in biomass gasification. *Catal. Commun.*, 8: 1697-1701.
- Sutton, D., B. Kelleher and J.R.H. Ross, 2001. Review of literature on catalyst for biomass gasification. *Fuel Process. Technol.*, 73: 155-173.
- Uddin, M.A., H. Tsuda and E. Sasaoka, 2008. Catalytic decomposition of biomass tars with iron oxide catalyst. *Fuel*, 87: 451-459.
- Virginie, M., S. Libs, A. Courson and A. Kiennemann, 2008. Iron/olivine catalysts for tar reforming: Comparison with nickel/olivine. <http://gdricatal.univ-lille1.fr/GDRI%20FR/21-28.pdf>
- Wan, H.J., B.S. Wu, C.H. Zhang, H.W. Xiang, Y.W. Li, B.F. Xu and F. Yi, 2007. Study of Fe- $\text{Al}_2\text{O}_3$  interaction over precipitated iron catalyst for fisher-tropsch synthesis. *Catal. Commun.*, 8: 1538-1545.
- Webb, P.A. and C. Orr, 1997. Analytical Methods in Fine Particle Technology. Micromeritics Instrument Corporation, Norcross, GA, USA.
- Wielers, A.F.H., A.J.H.M. Kock, C.E.C.A. Hop and J.W. Geus, 1989. The reduction behavior of silica-supported and alumina-supported iron catalysts: A mijsbauer and infrared spectroscopic study. *J. Catal.*, 117: 1-18.
- Zhang, C.H., Y. Yang, B.T. Teng, T.Z. Li, H.Y. Zheng, H.W. Xiang and Y.W. Li, 2006. Study of an iron-manganese fischer-tropsch synthesis catalyst promoted with copper. *J. Catal.*, 237: 405-415.
- Zhang, R., Y. Wang and R.C. Brown, 2007. Steam reforming of tar compounds over ni/olivine catalysts doped with  $\text{CeO}_2$ . *Energy Conv. Manage.*, 48: 68-77.
- Zielinski, J., 1982. Morphology of nickel/alumina catalysts. *J. Catal.*, 76: 157-163.